Nonlinear Dyn (2016) 86:911–926
DOI 10.1007/s11071-016-2932-9

ORIGINAL PAPER

Designing a terminal optimal control with an integral sliding mode component using a saddle point method approach: a Cartesian 3D-crane application

Cesar U. Solis · Julio B. Clempner · Alexander S. Poznyak

Received: 17 December 2015 / Accepted: 27 June 2016 / Published online: 8 July 2016

Abstract This paper proposes a new approach for designing a nonlinear optimal controller with an integral sliding mode component employing a generalization of the saddle point method which consists on controlling a controllable nonlinear system. Based on the initial and final conditions of the dynamical system, we consider an open-loop control such that the state of the system can be moved to a neighborhood of the equilibrium state corresponding to the given final condition. The implementation of the method for solving the problem involves a two-step iterated procedure: (i) The first step consists of a "prediction" which calculates the preliminary position approximation to the steady-state point, and (ii) the second step is designed to find a "basic adjustment" of the previous prediction. We apply the controller to a Cartesian 3D-crane. The formulation of the 3D-crane is in terms of nonlinear programming problems implementing the Lagrange principle. We transform the problem in a system of equations where each equation is itself an optimization problem. For designing the controller we suggest to employ an integral sliding mode method which suppress the model uncertainties consequence of moving the trolley and the bridge, lifting the cargo as well as external forces. As a result, the optimal controller will be simultaneously able to lift the cargo, suppressing the payload vibration, tracking the trolley and moving the bridge. A numerical example involving the simulation of a 3D-crane shows the effectiveness of the controller.

Keywords Optimal control · Integral sliding mode · 3D-crane · Saddle point method

C. U. Solis (✉)· A. S. Poznyak
Department of Control Automatics, Center for Research and Advanced Studies, Av. IPN 2508, Col. San Pedro Zacatenco, 07360 Mexico City, Mexico
e-mail: csolis@ctrl.cinvestav.mx

A. S. Poznyak
e-mail: apoznyak@ctrl.cinvestav.mx

J. B. Clempner
Centro de Investigaciones Economicas, Administrativas y Sociales, Instituto Politecnico Nacional, Lauro Aguirre 120, col. Agricultura, Miguel Hidalgo, 11360 Mexico City, Mexico
e-mail: julio@clempner.name

1 Introduction

1.1 Brief review

The *optimal control* deals with the process of finding a control and state trajectories for a dynamic system over a period of time until a certain optimality criterion is achieved [6]. In other words, an optimal control is a set of differential equations describing the paths of the control variables that minimize the cost of a given functional. It is usually solved using the Pontrya-

gin's maximum principle or by solving the Hamilton–Jacobi–Bellman equation. The *terminal optimal control* problem is the process of determining a control and state trajectories driving a dynamic system from an initial state to final state over a fixed finite time. The dynamic systems are assumed to be embedded in a constantly varying environment, and they are affected by its various factors. The environment is described by a controlled dynamics.

The integral sliding mode control (ISMC) is employed to compensate the uncertainties from the beginning of the process, and it was proposed in their seminal work by Utkin and Shi [29]. Interesting applications of ISMC can be found in [11,13,16,25,28,30,32–34]. In ISMC solution problem the order of the motion equation is equal to the order of the original dynamical system. Then, the trajectory for a system driven by a smooth control law can be guaranteed throughout an entire response of the system starting from the initial time instance. The implementation of this ISMC concept requires a priori knowledge of the state vector and the initial conditions. The optimal control problem in the presence of uncertainties was considered in [34]. They proposed the use of the integral sliding mode control allowing to ensure the robustness of the solution from the initial time moment.

The operation of a crane is an interesting terminal optimal control problem that involves from an initial position lift the payload, track the trolley and move the bridge simultaneously to a final state [8,26]. From the control point of view, it is required suppressing the uncertainties of stopping the trolley and the bridge at the destination position, as well as eliminating the external forces.

The mathematical model of the 3D-crane is a system of nonlinear ordinary differential equations, based on the Newton's law of motion, where the control represents the force of the motor [19]. Based on the initial and final conditions of the dynamical system, we consider an open-loop control such that the state of the system can be moved to a neighborhood of the equilibrium state corresponding to the given final condition. In addition, we consider an integral sliding mode method which suppress the model uncertainties consequence of moving the trolley and the bridge, as well as external forces. Then, our control solution scheme involves both, a terminal optimal open-loop control and a closed-loop sliding mode control.

1.2 Related work

Several solutions using different methods have been presented in the literature. For a survey see [14]. Several studies used classical methods for solving the problem. For instance, Algarni et al. [1] considered an overhead crane which represents simultaneous travel, traverse, and hoisting motions studying nonlinear feedback forms of control. Sakawa and Sano [24] suggested an overhead crane with an open-loop control and apply a feedback method so that the state of the system approaches the equilibrium state as quick as possible. Giua et al. [12] designed an observer/controller for three degrees of freedom overhead crane considering a linear model of the crane where the length of the suspending rope is a time-varying parameter.

Other methods employ fuzzy controllers like, and Chang and Chiang [7] presented a method based on the inertia theorem that uses trolley position and swing angle data to design the proposed fuzzy projection controller and employed an enhanced fuzzy algorithm to eliminate the dead zone problem. Cho and Lee [9] proposed a fuzzy antiswing control for a three-dimensional overhead crane consisting of a position servo control and a fuzzy-logic control.

Related researches using sliding mode control for overhead crane systems have also been published since its introduction. Karkoub and Zribi [15] presented to control the overhead crane a variable structure control scheme, a variable structure controller in conjunction with a state feedback control scheme, and a μ-synthesis control scheme. Bartolini et al. [4] proposed a second-order sliding modes, which guarantees a fast and precise load transfer and the swing suppression during the load movement, despite model uncertainties and unmodeled dynamic actuators. Bartolini et al. [5] compared the second-order sliding mode controller presented in [4] with (i) the smooth approximation of a first-order sliding mode controller; (ii) an observer/controller scheme based on Lyapunov transformations; and (iii) a classical PID controller. Park et al. [21] suggested an adaptive fuzzy sliding mode control for the robust antisway trajectory tracking of overhead cranes subject to both system uncertainty and actuator nonlinearity. Liu et al. [18] presented an adaptive sliding mode fuzzy control approach for a two-dimensional overhead crane combining the sliding mode control robustness and the feedback linear control independence of the system model. Lee et al. [17]

considered a sliding mode antiswing control for overhead cranes based on the Lyapunov stability theorem, where a sliding surface, coupling the trolley motion with load swing, is adopted for a direct damping control of load swing ensuring asymptotic stability while keeping all internal signals bounded. Daqaq and Masoud [10] developed a two-dimensional four-bar-mechanism model of a container crane reduced to a double pendulum with two fixed-length links and a kinematic constraint. Almutairi and Zribi [2] proposed a sliding mode control for a three-dimensional overhead crane which ensures the asymptotic stability of the closed-loop system. Ngo and Hong [20] proposed a sliding mode control for an offshore container crane used to load/unload containers between a huge container ship and a smaller ship, on which the crane is installed, and it is also presented a mechanism for lateral sway control ensuring the asymptotic stability of the closed-loop system. Wu et al. [31] considered an approach that minimize an objective function that is formulated as the integration of energy consumption and swing angle for energy efficiency as well as safety. Sun et al. [27] considered the control problem for underactuated crane systems where the control framework is established by total energy shaping, and a novel additional term is introduced into the controller to prevent the trolley from running out of the permitted range. Qian et al. [23] addressed the dynamics and trajectory tracking control of cooperative multiple mobile cranes providing a theoretical basis for the cooperation of multiple mobile cranes.

1.3 Main results

This paper makes the following contributions:

- We suggest a generalization of saddle point method [3] for nonlinear and controllable dynamical systems.
- We propose an optimal terminal control for a 3D-crane employing the generalized saddle point method.
- We introduce an integral sliding mode control which suppress the model uncertainties consequence of moving the trolley, the bridge, lifting the cargo and external forces.
- We prove that the method converges to an steady-state function.
- We present a numerical example involving the simulation of a 3D-crane that validates the effectiveness of the controller.

1.4 Organization of the paper

The remainder of this paper is organized as follows. The next section discusses and presents the motivating problem. Section 3 suggests the optimization method presenting the dynamics of the problem, the conditions for optimality, and a generalization of saddle point method [3]. Section 4 presents the implementation of the saddle point method for the Cartesian 3D-crane describing the dynamical model and a numerical example, as well as the design of the optimal terminal control. We design an integral sliding mode control to compensate the uncertainties and present an application example for the Cartesian 3D-crane in Sect. 5. Finally, Sect. 6 concludes and discusses future work.

2 Formulation of the problem

In this paper our main purpose is to obtain an optimal control [6] arising whenever the state of a system at time $0 \leq t \leq t_f$ as described by a vector

$$\mathbf{x}(t) = (x_1(t), \ldots, x_n(t))^{\mathsf{T}} \in \mathbb{R}^n$$

evolves according to a prescribed law, usually given in the form of a first-order vector ordinary differential equation

$$\dot{\mathbf{x}}(t) = f\,(\mathbf{x}(t), \mathbf{u}(t))$$

under the assignment of a vector-valued control function

$$\mathbf{u}(t) = (u_1(t), \ldots, u_r(t))^{\mathsf{T}} \in \mathbb{R}^r$$

which is the control that may run over a given control region $U \subset L_2^r\left[t_0, t_f\right]$ (L_2^r are the integrable quadratic functions of dimension r). On the right-hand side, where

$$f\,(\mathbf{x}(t), \mathbf{u}(t)) = (f_1(\mathbf{x}(t), \mathbf{u}(t)), \ldots, f_n\,(\mathbf{x}(t), \mathbf{u}(t)))^{\mathsf{T}} \in \mathbb{R}^n$$

we impose the usual restrictions: continuity with respect to the arguments $\mathbf{x}(t)$ and $\mathbf{u}(t)$, measurability on t, and differentiability (or the Lipschitz condition) with respect to $\mathbf{x}(t)$. Here we will assume that the admissible $\mathbf{u}(t)$ may be only piecewise continuous at each time interval from $0 \leq t \leq t_f$ (t is allowed to vary). Controls that have the same values except at common points of discontinuity will be considered as identical.

Formally, the terminal optimal control problem is the process of computing a fixed point of an extremal mapping. This means finding a fixed point

$$\mathbf{x}_0^* \in \operatorname{Arg\,min} \left\{ \varphi_0 (\mathbf{x}_0) \,|\mathbf{x}_0 \in W_0 \subset \mathbb{R}^n \right\} \tag{1}$$

$$\begin{aligned} &\mathbf{x}_1^* \in \operatorname{Arg\,min} \left\{ \varphi_1 (\mathbf{x}_1) \,|\mathbf{x}_1 \in W_1 \subset \mathbb{R}^n, \right. \\ &\dot{\mathbf{x}}(t) = f(\mathbf{x}(t), \mathbf{u}(t)), \mathbf{x}(0) = \mathbf{x}_0^*, \\ &\left. \mathbf{x}\left(t_f\right) = \mathbf{x}_1^*,\ 0 \le t \le t_f,\ \mathbf{u}(t) \in U_{\text{adm}} \right\} \end{aligned} \tag{2}$$

where $\mathbf{x}(t)$ and $\mathbf{u}(t)$ are the state trajectories and the control, respectively, $\mathbf{x}_0 = \mathbf{x}(0)$ and $\mathbf{x}_1 = \mathbf{x}\left(t_f\right)$ describe the set of initial and terminal conditions, $\varphi_0(\cdot)$ and $\varphi_1(\cdot)$ are a convex functions, $W_0, W_1 \subset \mathbb{R}^n$ are convex closed bounded sets, and U_{adm} is a convex closed set of admissible control actions $\mathbf{u}(t)$ for the dynamic system. The fixed points of extremal inclusions given in Eqs. (1) and (2) are the initial and terminal conditions $\mathbf{x}_0 = \mathbf{x}(0)$ and $\mathbf{x}_1 = \mathbf{x}\left(t_f\right)$ of dynamical system.

Remark 1 We consider the controlled dynamics given by a system of linear differential equations. The initial and terminal conditions of this system are set implicitly.

The solving process given in Eqs. (1) and (2) is as follows. Choosing a control $\mathbf{u}(t) \in U_{\text{adm}}$ and an initial condition $\mathbf{x}_0 = \mathbf{x}(0)$ we solve differential system $\dot{\mathbf{x}}(t) = f(\mathbf{x}(t), \mathbf{u}(t))$ to find a unique trajectory $\mathbf{x}(t)$. The trajectory has an initial and terminal conditions $\mathbf{x}_0 = \mathbf{x}(0)$ and $\mathbf{x}_1 = \mathbf{x}\left(t_f\right)$. Then, we verify $\mathbf{x}_0 = \mathbf{x}(0)$ and $\mathbf{x}_1 = \mathbf{x}\left(t_f\right)$ are solutions of boundary value problems given in Eqs. (1) and (2). Otherwise, we look for different initial and terminal conditions. As a result of finding an optimal control $\mathbf{u}^*(t) \in U_{adm}$, the trajectory $\mathbf{x}^*(t)$ as a solution of differential system $\dot{\mathbf{x}}(t) = f(\mathbf{x}(t), \mathbf{u}(t))$ transfers the dynamical system from initial state given in Eq. (1) to a terminal state in Eq. (2).

3 Optimization solution method

3.1 Dynamic problem

We will specify the dynamic problem presented in Eqs. (1) and (2) considering the case where the finite-dimensional sets $W_0, W_1 \subset \mathbb{R}^n$ are defined by the following functional inequality constraints

$$\mathbf{x}_0^* \in \operatorname{Arg\,min} \{ \varphi_0 (\mathbf{x}_0) \,|A_0 \mathbf{x}_0 \le a_0 \} \tag{3}$$

$$\begin{aligned} &\mathbf{x}_1^* \in \operatorname{Arg\,min} \{ \varphi_1 (\mathbf{x}_1) \,|A_1 \mathbf{x}_1 \le a_1, \\ &\dot{\mathbf{x}}(t) = f(\mathbf{x}(t), \mathbf{u}(t)), \mathbf{x}(0) = \mathbf{x}_0^*, \\ &\mathbf{x}\left(t_f\right) = \mathbf{x}_1^*,\ 0 \le t \le t_f, \mathbf{u}(t) \in U_{\text{adm}} \} \end{aligned} \tag{4}$$

where A_0 and A_1 are fixed matrices that represent algebraically the convex region of convergence of the initial and final points, respectively, and a_0 and a_1 are given vectors.

Let us consider that the dynamical system is given in Eqs. (3) and (4) in a Hilbert space. That is, up to a null set, all the values of the control function $u(\cdot)$ belong to the set U. If the controls range over the entire set $u(\cdot) \in U$, the differential system given in Eq. (4) generates trajectories $\mathbf{x}(t), 0 \le t \le t_f$, whose extremal points $\mathbf{x}(0) = \mathbf{x}_0^*$ and $\mathbf{x}\left(t_f\right) = \mathbf{x}_1^*$ describe the set of initial and terminal conditions.

The process given in Eqs. (3) and (4) is as follows. The linear controlled system $\dot{\mathbf{x}}(t) = f(\mathbf{x}(t), \mathbf{u}(t))$ is a linear constraint that singles out a linear manifold of functions (processes) $(\mathbf{x}(t), \mathbf{u}(t))$ defined on the interval $\left[0, t_f\right]$. The left and right ends $(\mathbf{x}(0) = \mathbf{x}_0^*,\ \mathbf{x}\left(t_f\right) = \mathbf{x}_1^*)$ of the trajectories generate a set on $\mathbb{R}^n$. The function φ_0 and φ_1 as well the sets $W_i = \{\mathbf{x}_i \in \mathbb{R}^n | A_i \mathbf{x}_i \le a_i\}$, $i = 0, 1$, are defined on $\mathbb{R}^n$. For these components, the problems of computing fixed points of extremal mappings are stated. An optimal control $\mathbf{u}^*(t) \in U_{\text{adm}}$ has to be chosen so that the trajectory $\mathbf{x}^*(t)$ joins the points $\mathbf{x}(0) = \mathbf{x}_0^*$ and $\mathbf{x}\left(t_f\right) = \mathbf{x}_1^*$ [transfers the dynamical system from initial state given in Eq. (3) to a terminal state in Eq. (4)].

Note that, in this situation, the initial and terminal conditions given by $\mathbf{x}(0) = \mathbf{x}_0^*$ and $\mathbf{x}\left(t_f\right) = \mathbf{x}_1^*$ are not related by additional constraints and the two problems can be solved sequentially. However, the method we propose constructs a sequence of trajectories starting at different initial points, but this sequence of initial points converges to the solution of problem given in Eq. (3) simultaneously.

Remark 2 The terminal optimal control has no restrictions along the trajectory. We have restrictions only in the initial $\mathbf{x}(0)$ an final point $\mathbf{x}\left(t_f\right)$.

3.2 Optimality condition

To solve the optimization problem (1)–(2) let us apply the Lagrange multiplier method [22] as follows

$$\mathcal{L}\left(\mathbf{x}_0, \mathbf{x}_1, \mathbf{x}(t), \mathbf{u}(t); p_0, p_1, \Psi(t)\right) := \varphi_0\left(\mathbf{x}_0\right) + \varphi_1\left(\mathbf{x}_1\right) + \langle p_0, A_0\mathbf{x}_0 - a_0\rangle + \langle p_1, A_1\mathbf{x}_1 - a_1\rangle + \langle \Psi(t), f\left(\mathbf{x}(t), \mathbf{u}(t)\right)\rangle$$

given $p_0, p_1 \in \mathbb{R}^m_+$, $\Psi(t)$ the co-state of $\mathbf{x}(t)$, where $\langle\cdot,\cdot\rangle$ represents the standard inner product on a Hilbert space. In the regular case, such a function always has a saddle point $\left(\mathbf{x}_0^*, \mathbf{x}_1^*, \mathbf{x}^*(t), \mathbf{u}^*(t); p_0^*, p_1^*, \Psi^*(t)\right)$ satisfying the system of inequalities

$$\begin{aligned}&\mathcal{L}\left(\mathbf{x}_0^*, \mathbf{x}_1^*, \mathbf{x}^*(t), \mathbf{u}^*(t); p_0, p_1, \Psi(t)\right)\\ &\le \mathcal{L}\left(\mathbf{x}_0^*, \mathbf{x}_1^*, \mathbf{x}^*(t), \mathbf{u}^*(t); p_0^*, p_1^*, \Psi^*(t)\right)\\ &\le \mathcal{L}\left(\mathbf{x}_0^*, \mathbf{x}_1^*, \mathbf{x}(t), \mathbf{u}(t); p_0^*, p_1^*, \Psi^*(t)\right)\end{aligned}$$

Here, $\left(\mathbf{x}_0^*, \mathbf{x}_1^*, \mathbf{x}^*(t), \mathbf{u}^*(t); p_0^*, p_1^*, \Psi^*(t)\right)$ is the collection of vectors solving system given in Eqs. (1)–(2).

Applying the maximum principle, which gives the necessary conditions of optimality, yields:

$$\begin{aligned}&\dot{\mathbf{x}}(t) = \frac{\partial\mathcal{L}}{\partial\Psi} = f\left(\mathbf{x}(t), \mathbf{u}(t)\right)\\ &\dot{\Psi}(t) = -\frac{\partial\mathcal{L}}{\partial\mathbf{x}} = -\frac{\partial f\left(\mathbf{x}(t), \mathbf{u}(t)\right)}{\partial\mathbf{x}}^{\mathsf{T}}\Psi(t)\\ &0 = \frac{\partial f\left(\mathbf{x}(t), \mathbf{u}(t)\right)}{\partial\mathbf{u}}^{\mathsf{T}}\Psi(t)\\ &\Psi_1 = \nabla\varphi_1\left(\mathbf{x}_1\right) + A_1^{\mathsf{T}}p_1\\ &\Psi_0 = -\nabla\varphi_0\left(\mathbf{x}_0\right) - A_0^{\mathsf{T}}p_0\end{aligned}$$

and the inequalities

$$\begin{aligned}&\langle p_0, A_0\mathbf{x}_0 - a_0\rangle \le 0\\ &\langle p_1, A_1\mathbf{x}_1 - a_1\rangle \le 0\end{aligned}$$

Then reordering and applying variational inequalities we have

$$\begin{aligned}&\dot{\mathbf{x}}^*(t) = f(\mathbf{x}^*(t), \mathbf{u}^*(t)),\ \mathbf{x}^*(0) = \mathbf{x}_0^*,\\ &\left\langle p_0 - p_0^*, A_0\mathbf{x}_0^* - a_0\right\rangle \le 0,\\ &\left\langle p_1 - p_1^*, A_1\mathbf{x}_1^* - a_1\right\rangle \le 0,\\ &\dot{\Psi}^*(t) + \frac{\partial f\left(\mathbf{x}^*(t), \mathbf{u}^*(t)\right)}{\partial\mathbf{x}}^{\mathsf{T}}\Psi^*(t) = 0,\\ &\Psi_1^* = \nabla\varphi_1\left(\mathbf{x}_1^*\right) + A_1^{\mathsf{T}}p_1^*,\\ &\nabla\varphi_0\left(\mathbf{x}_0^*\right) + A_0^{\mathsf{T}}p_0^* + \Psi_0^* = 0,\\ &\left\langle\frac{\partial f\left(\mathbf{x}^*(t), \mathbf{u}^*(t)\right)}{\partial\mathbf{u}}^{\mathsf{T}}\Psi^*(t), \mathbf{u}^*(t) - \mathbf{u}(t)\right\rangle \le 0\end{aligned} \tag{5}$$

The variational inequalities of the system (5) can be rewritten in an equivalent form as operator equations with projectors onto the corresponding convex closed sets. Then, we obtain a system of differential and operator equations of the form

$$\dot{\mathbf{x}}^*(t) = f(\mathbf{x}^*(t), \mathbf{u}^*(t)),\ \mathbf{x}^*(0) = \mathbf{x}_0^* \tag{6}$$

$$\begin{aligned}&p_0^* = \pi_+\left(p_0^* + \epsilon\left(A_0\mathbf{x}_0^* - a_0\right)\right)\\ &p_1^* = \pi_+\left(p_1^* + \epsilon\left(A_1\mathbf{x}_1^* - a_1\right)\right)\end{aligned} \tag{7}$$

$$\dot{\Psi}^*(t) + \frac{\partial f\left(\mathbf{x}^*(t), \mathbf{u}^*(t)\right)}{\partial\mathbf{x}}^{\mathsf{T}}\Psi^*(t) = 0$$

$$\Psi_1^* = \nabla\varphi_1\left(\mathbf{x}_1^*\right) + A_1^{\mathsf{T}}p_1^* \tag{8}$$

$$\mathbf{u}^*(t) = \pi_U\left(\mathbf{u}^*(t) - \epsilon\frac{\partial f\left(\mathbf{x}^*(t), \mathbf{u}^*(t)\right)}{\partial\mathbf{u}}^{\mathsf{T}}\Psi^*(t)\right) \tag{9}$$

$$\nabla\varphi_0\left(\mathbf{x}_0^*\right) + A_0^{\mathsf{T}}p_0^* + \Psi_0^* = 0 \tag{10}$$

where $\pi_+(\cdot)$ is the projectors onto the positive orthant of $\mathbb{R}^n$, and π_U is the projectors onto the set $U_{\text{adm}}, \epsilon > 0$.

3.3 Saddle point optimization method

The dynamical system presented in Eqs. (6)–(10) is used to develop a gradient projection method given by

$$\dot{\mathbf{x}}^k(t) = f\left(\mathbf{x}^k(t), \mathbf{u}^k(t)\right),\ \mathbf{x}^k(0) = \mathbf{x}_0^k \tag{11}$$

$$\begin{aligned}&p_0^{k+1} = \pi_+\left(p_0^k + \epsilon\left(A_0\mathbf{x}_0^k - a_0\right)\right)\\ &p_1^{k+1} = \pi_+\left(p_1^k + \epsilon\left(A_1\mathbf{x}_1^k - a_1\right)\right)\end{aligned} \tag{12}$$

$$\dot{\Psi}^k(t) + \frac{\partial f\left(\mathbf{x}^k(t), \mathbf{u}^k(t)\right)}{\partial\mathbf{x}}^{\mathsf{T}}\Psi^k(t) = 0$$

$$\Psi_1^k = \nabla\varphi_1\left(\mathbf{x}_1^k\right) + A_1^{\mathsf{T}}p_1^k \tag{13}$$

$$\mathbf{u}^{k+1}(t) = \pi_U\left(\mathbf{u}^k(t) - \epsilon\frac{\partial f\left(\mathbf{x}^k(t), \mathbf{u}^k(t)\right)}{\partial\mathbf{u}}^{\mathsf{T}}\Psi^k(t)\right) \tag{14}$$

$$\mathbf{x}_0^{k+1} = \mathbf{x}_0^k - \epsilon\left(\nabla\varphi_0\left(\mathbf{x}_0^k\right) + A_0^{\mathsf{T}}p_0^k + \Psi_0^k\right) \tag{15}$$

where k is the number of the iteration.

Each iteration is, in fact, reduced to solve two systems of differential equations (11) and (13). The condition (13) holds at points of the reachable set.

However, computing a saddle point requires a different solution process, because in the case of the computing the neighborhood of a saddle point implies that the iteration splits into two-half-step iteration process which transfer from an orbit of large radius to an orbit with a smaller distance to the fixed point.

Then, the saddle point process has the following form [3]:

1. First half step (prediction)

$$\dot{\mathbf{x}}^k(t) = f\left(\mathbf{x}^k(t), \mathbf{u}^k(t)\right),\ \mathbf{x}^k(0) = \mathbf{x}_0^k \tag{16}$$

$$\bar{p}_0^k = \pi_+\left(p_0^k + \epsilon\left(A_0\mathbf{x}_0^k - a_0\right)\right)$$

$$\bar{p}_1^k = \pi_+\left(p_1^k + \epsilon\left(A_1\mathbf{x}_1^k - a_1\right)\right) \tag{17}$$

$$\dot{\Psi}^k(t) + \frac{\partial f\left(\mathbf{x}^k(t), \mathbf{u}^k(t)\right)}{\partial \mathbf{x}}^{\mathsf{T}} \Psi^k(t) = 0$$

$$\Psi_1^k = \nabla\varphi_1\left(\mathbf{x}_1^k\right) + A_1^{\mathsf{T}} p_1^k \tag{18}$$

$$\bar{\mathbf{u}}^k(t) = \pi_U\left(\mathbf{u}^k(t) - \epsilon\frac{\partial f\left(\mathbf{x}^k(t), \mathbf{u}^k(t)\right)}{\partial \mathbf{u}}^{\mathsf{T}} \Psi^k(t)\right) \tag{19}$$

$$\bar{\mathbf{x}}_0^k = \mathbf{x}_0^k - \epsilon\left(\nabla\varphi_0\left(\mathbf{x}_0^k\right) + A_0^{\mathsf{T}} p_0^k + \Psi_0^k\right) \tag{20}$$

2. Second half step (refinement):

$$\dot{\bar{\mathbf{x}}}^k(t) = f\left(\bar{\mathbf{x}}^k(t), \bar{\mathbf{u}}^k(t)\right),\ \bar{\mathbf{x}}^k(0) = \bar{\mathbf{x}}_0^k \tag{21}$$

$$p_0^{k+1} = \pi_+\left(p_0^k + \epsilon\left(A_0\bar{\mathbf{x}}_0^k - a_0\right)\right)$$

$$p_1^{k+1} = \pi_+\left(p_1^k + \epsilon\left(A_1\bar{\mathbf{x}}_1^k - a_1\right)\right) \tag{22}$$

$$\dot{\bar{\Psi}}^k(t) + \frac{\partial f\left(\bar{\mathbf{x}}^k(t), \bar{\mathbf{u}}^k(t)\right)}{\partial \bar{\mathbf{x}}}^{\mathsf{T}} \bar{\Psi}^k(t) = 0$$

$$\bar{\Psi}_1^k = \nabla\varphi_1\left(\bar{\mathbf{x}}_1^k\right) + A_1^{\mathsf{T}} \bar{p}_1^k \tag{23}$$

$$\mathbf{u}^{k+1}(t) = \pi_U\left(\mathbf{u}^k(t) - \epsilon\frac{\partial f\left(\bar{\mathbf{x}}^k(t), \bar{\mathbf{u}}^k(t)\right)}{\partial \bar{\mathbf{u}}}^{\mathsf{T}} \bar{\Psi}^k(t)\right) \tag{24}$$

$$\mathbf{x}_0^{k+1} = \mathbf{x}_0^k - \epsilon\left(\nabla\varphi_0\left(\bar{\mathbf{x}}_0^k\right) + A_0^{\mathsf{T}} \bar{p}_0^k + \bar{\Psi}_0^k\right) \tag{25}$$

Following [3], we suggest the next generalized theorem.

Theorem 1 *Assume that the solution*

$$\left(p_0^*, p_1^*, \Psi^*(\cdot); \mathbf{x}_0^*, \mathbf{x}_1^*, \mathbf{x}^*(\cdot), \mathbf{u}^*(\cdot)_0^k, \bar{\Psi}_0^k\right) \tag{26}$$

of problem given in Eqs. (3) and (4) is not empty and belongs to the space $\mathbb{R}_+^m \times \mathbb{R}_+^m \times \Psi_2^n[t_0, t_1] \times \mathbb{R}^n \times \mathbb{R}^n \times \overline{AC}^n[t_0, t_1] \times U_{\text{adm}}$ *such that* $\|\frac{\partial f}{\partial \mathbf{u}}\|$ *and* $\|\frac{\partial f}{\partial \mathbf{x}}\|$ *are bounded, and let the terminal problems at the left and right endpoints of the time interval be problems of computing fixed points of monotone extremal mappings. Then, the sequence* $\left(p_0^k, p_1^k, \Psi^k(\cdot); \mathbf{x}_0^k, \mathbf{x}_1^k, \mathbf{x}^k(\cdot), \mathbf{u}^k(\cdot)\right)$ *generated by the saddle point process given by Eqs. (16)–(25) with the step size determined by the condition* $0 < \epsilon < \epsilon_0$ *(*ϵ_0 *is a fixed number) converges weakly to the solution of the problem with respect to controls, in the* $L_2^r[t_0, t_1]$ *norm, and with respect to trajectories and dual trajectories, and converges in the Euclidean norm to the solutions of the terminal problems at the endpoints of the time interval. Moreover, the sequence*

$$\left\{\left\|\mathbf{u}^k(\cdot) - \mathbf{u}^*(\cdot)\right\|^2 + \left|p_0^k - p_0^*\right|^2 + \left|p_1^k - p_1^*\right|^2 + \left|\mathbf{x}_0^k - \mathbf{x}_0^*\right|^2\right\}$$

decreases monotonically as $k \to \infty$. *By the dynamical system condition of the crane* $\|\frac{\partial f}{\partial \mathbf{u}}\|$ *and* $\|\frac{\partial f}{\partial \mathbf{x}}\|$ *are bounded.*

Proof See "Appendix." □

4 Saddle point method for the Cartesian 3D-crane

4.1 Dynamical model

A Cartesian 3D-crane is composed by two components: the bridge and the trolley. The trolley moves on the bridge rails and contains a motor and all the necessary mechanisms for the movement of the load; the bridge moves in the orthogonal direction thanks to appropriate wheels located on the end truck. In this paper, we will consider a Cartesian 3D overhead crane whose model is illustrated in Fig. 1.

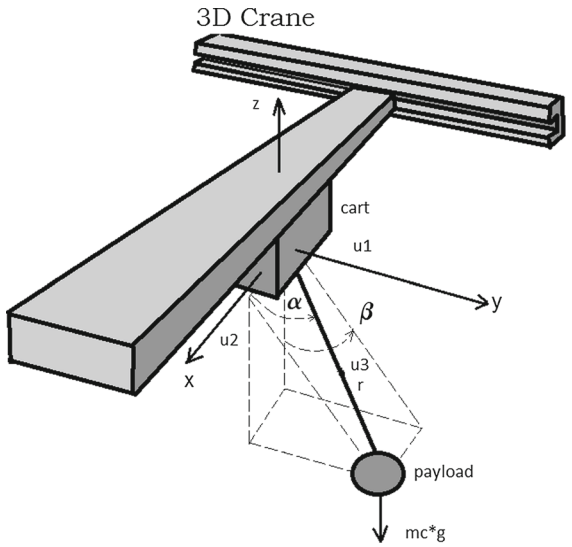

Fig. 1 Illustrative representation of a Cartesian 3D-crane

First, we will develop the physical model of Euler–Lagrange. Let us consider the Lagrange equation given by:

$$\mathcal{L}(\mathbf{x}) := E_k - E_p \tag{27}$$

where $\mathbf{x} = \left(x_w, \dot{x}_w, y_w, \dot{y}_w, \alpha, \dot{\alpha}, \beta, \dot{\beta}, r, \dot{r}\right)$, x_w and y_w are the planar coordinates of the trolley, $\dot{x}_w$ and $\dot{y}_w$ represent the linear velocities, respectively, the angle α $(0 \leq \alpha \leq \pi)$ is measured from the positive x-axis to the tension line of the payload (r-axis), the angle β $(-\pi/2 \leq \beta \leq \pi/2)$ is measured from the negative z-axis to the projection of the tension line onto the y–z plane, $\dot{\alpha}$ and $\dot{\beta}$ are the corresponding angular velocities, and, finally, $r > 0$ is the radial coordinate of the payload (measure from the trolley) and $\dot{r}$ its velocity.

E_k represents the total kinetic energy of the system, and E_p is the potential energy. The kinetic energy for the trolley is given by

$$E_{k_1} = \frac{1}{2} m_w \left(\dot{x}_w^2 + \dot{y}_w^2\right)$$

where m_w is the mass of the trolley. For determining the kinetic energy of the payload, we consider the following coordinate equations

$$\begin{aligned} x_c &= x_w + r\cos\alpha \\ y_c &= y_w + r\sin\alpha\sin\beta \\ z_c &= -r\sin\alpha\cos\beta \end{aligned}$$

then, taking the derivatives with respect to the time we have

$$\begin{aligned} \dot{x}_c &= \dot{x}_w + \dot{r}\cos\alpha - r\dot{\alpha}\sin\alpha \\ \dot{y}_c &= \dot{y}_w + \dot{r}\sin\alpha\sin\beta + r\dot{\alpha}\cos\alpha\sin\beta + r\dot{\beta}\sin\alpha\cos\beta \\ \dot{z}_c &= -\dot{r}\sin\alpha\cos\beta - r\dot{\alpha}\cos\alpha\cos\beta + r\dot{\beta}\sin\alpha\sin\beta \end{aligned}$$

We have that the kinetic energy of the payload is as follows

$$E_{k_2} = \frac{1}{2} m_c \left(\dot{x}_c^2 + \dot{y}_c^2 + \dot{z}_c^2\right) \tag{28}$$

As a result, the total energy of the system is given by

$$E_k = E_{k_1} + E_{k_2}$$

The potential energy of the trolley is cero, while the potential energy of the payload is given by

$$E_{p_2} = m_c g z_c$$

then, the Lagrange equation (27) can be reduced to

$$\begin{aligned} \mathcal{L}\left(x_w, \dot{x}_w, y_w, \dot{y}_w, \alpha, \dot{\alpha}, \beta, \dot{\beta}, r, \dot{r}\right) = {} & \frac{1}{2} m_c \cdot \\ & \Big[\left(\dot{y}_w + \dot{r}\sin\alpha\sin\beta + \dot{\alpha} r\cos\alpha\sin\beta + \dot{\beta} r\cos\beta\sin\alpha\right)^2 \\ & + \left(\dot{r}\cos\beta\sin\alpha + \dot{\alpha} r\cos\alpha\cos\beta - \dot{\beta} r\sin\alpha\sin\beta\right)^2 \\ & + \left(\dot{x}_w + \dot{r}\cos\alpha - \dot{\alpha} r\sin\alpha\right)^2\Big] \\ & + \frac{1}{2} m_w \left(\dot{x}_w^2 + \dot{y}_w^2\right) + m_c g r\cos\beta\sin\alpha \end{aligned}$$

Applying the Euler–Lagrange equations we have

$$\frac{\mathrm{d}}{\mathrm{d}t}\left(\frac{\partial \mathcal{L}}{\partial \dot{\mathbf{x}}}\right) - \frac{\partial \mathcal{L}}{\partial \mathbf{x}} + \frac{\partial \mathcal{R}}{\partial \dot{\mathbf{x}}} = \mathcal{F} \tag{29}$$

where $\mathbf{x} = \begin{bmatrix} x_w & \dot{x}_w & y_w & \dot{y}_w & \alpha & \dot{\alpha} & \beta & \dot{\beta} & r & \dot{r} \end{bmatrix}^\mathsf{T}$, and the vector $\mathcal{F} = \begin{bmatrix} u_1 & u_2 & 0 & 0 & -u_3 \end{bmatrix}^\mathsf{T}$ such that the first two components (u_1 and u_2) are the control forces over the trolley on the direction x and y, respectively, and the last component (u_3) is the control force over the payload. The sign $-$ (u_3) indicates the force is in negative sense of the r-axis direction, and this force compensates the weight of the payload. $\mathcal{R}$ is the Rayleigh's dissipation function, which is not considered along the development, i.e., we will not consider the friction force over the components of the 3D-crane.

From Eq. (29) we obtain the dynamical equations that describe the 3D-crane as follows

$$\ddot{x}_w = \frac{1}{m_w}\left[u_1 + u_3\cos\alpha\right] \tag{30}$$

$$\ddot{y}_w = \frac{1}{m_w}\left[u_2 + u_3\sin\alpha\sin\beta\right] \tag{31}$$

$$\begin{aligned} \ddot{\alpha} = {} & \frac{1}{m_w r}\Big[u_1\sin\alpha - u_2\cos\alpha\sin\beta - 2m_w\dot{\alpha}\dot{r} \\ & + \frac{1}{2}u_3\sin(2\alpha)\cos^2\beta \\ & + m_w g\cos\alpha\cos\beta + \frac{1}{2}m_w r\dot{\beta}^2\sin(2\alpha)\Big] \end{aligned} \tag{32}$$

$$\begin{aligned} \ddot{\beta} = {} & -\frac{1}{m_w r\sin\alpha}\Big[u_2\cos\beta + m_w g\sin\beta \\ & + \frac{1}{2}u_3\sin\alpha\sin(2\beta) + 2m_w\dot{\beta}\dot{r}\sin\alpha \\ & + 2m_w r\dot{\alpha}\dot{\beta}\cos\alpha\Big] \end{aligned} \tag{33}$$

$$\begin{aligned} \ddot{r} = {} & \frac{1}{m_w m_c}\Big[\left(m_c + m_w\right)u_3 + m_c u_1\cos\alpha \\ & - m_c u_3\cos^2\beta - m_c m_w r\left(\dot{\alpha}^2 + \dot{\beta}^2\right) \\ & + m_c u_3\cos^2\alpha\cos^2\beta + m_c u_2\sin\alpha\sin\beta \\ & - m_c m_w g\cos\beta\sin\alpha + m_c m_w r\dot{\beta}^2\cos^2\alpha\Big] \end{aligned} \tag{34}$$

4.2 Numerical example: terminal control

Given Eqs. (30)–(34) for the Cartesian 3D-crane, let us suppose we have the following conditions

$$t_f = 20[\text{s}]$$
$$m_c = 5[\text{kg}]$$
$$m_w = 5[\text{kg}]$$
$$g = 9.81[m/s^2]$$
$$|u_1| \leq (m_c + m_w)\, g[N]$$
$$|u_2| \leq (m_c + m_w)\, g[N]$$
$$|u_3| \leq (m_c + m_w)\, g[N]$$

The term $\mathbf{x}_s = [x_1, \ldots, x_n]^\intercal \pm y$ means that $x_i \pm y$ where $y \in \mathbb{R}_+$ and $i = 1, \ldots, n$ ($\mathbf{x}_s = [x_1 \pm y, \ldots, x_n \pm y]^\intercal$). This a vector centered in the coordinates $x_1, \ldots, x_n$ which admits a tolerance of $\pm y$ in every x_i, $i = 1, \ldots, n$. Let us also suppose that the initial and final state must satisfy the following restrictions:

$$\mathbf{x}_0 = \left[0\ 0\ 0\ 0\ \pi/2\ 0\ 0\ 0\ 10\ 0\right]^\intercal \pm 0.1$$
$$\mathbf{x}_1 = \left[10\ 0\ 15\ 0\ \pi/2\ 0\ 0\ 0\ 20\ 0\right]^\intercal \pm 1.0$$

for $\mathbf{x}_1$ we have $x_w \in (9, 11)$, $\dot{x}_w \in (-1, 1)$, $y_w \in (14, 16)$, $\dot{y}_w \in (-1, 1)$, $\alpha \in (\pi/2 - 1, \pi/2 + 2)$, $\dot{\alpha} \in (-1, 1)$, $\beta \in (-1, 1)$, $\dot{\beta} \in (-1, 1)$, $r \in (21, 19)$, $\dot{r} \in (-1, 1)$. The variables α and β are given in [rad], $\dot{\alpha}$ and $\dot{\beta}$ in [rad/s], and the rest in $[m]$ or $[m/s]$ depending on the case. We have a similar case for $\mathbf{x}_0$.

The matrices A_0 and A_1 are given by

$$A_0 = A_1 := \begin{bmatrix} AA_1 \\ \vdots \\ AA_{10} \end{bmatrix}$$

where

$$AA_j = \begin{bmatrix} \mathbf{0} \cdots \underbrace{\begin{bmatrix} 1 \\ -1 \end{bmatrix}}_{j} \cdots \mathbf{0} \end{bmatrix}$$

the vectors a_0 and a_1 are given by

$$a_0 := \left[0.1\ 0.1\ 0.1\ 0.1\ 0.1\ 0.1\ 0.1\right.$$
$$0.1\ \tfrac{\pi}{2} + 0.1\ 0.1 - \tfrac{\pi}{2}\ 0.1\ 0.1\ 0.1$$
$$\left.0.1\ 0.1\ 0.1\ 10.1\ -9.9\ 0.1\ 0.1\right]^\intercal$$

$$a_1 := \left[11\ -9\ 1\ 1\ 16\ -14\ 1\ 1\ \tfrac{\pi}{2} + 1\right.$$
$$\left.1 - \tfrac{\pi}{2}\ 1\ 1\ 1\ 1\ 1\ 1\ 21\ -19\ 1\ 1\right]^\intercal$$

and the cost functionals are defined as follows

$$\varphi_0\left(x\left(0\right)\right) := \tfrac{1}{2}\mathbf{x}^\intercal\left(0\right) Q_0 \mathbf{x}\left(0\right)$$
$$\varphi_1\left(x\left(t_f\right)\right) := \tfrac{1}{2}\left(\mathbf{x}\left(t_f\right) - \mathbf{r}\right)^\intercal Q_1 \left(\mathbf{x}\left(t_f\right) - \mathbf{r}\right)$$

where $\mathbf{r} = \left[10\ 0\ 15\ 0\ \pi/2\ 0\ 0\ 0\ 20\ 0\right]^\intercal$ and $Q_0 := \mathbf{I}_{10\times 10}$ and $Q_1 := \mathbf{I}_{10\times 10}$ where $\mathbf{I}_{10\times 10}$ is the identity matrix of order 10.

The goal is to simulate a terminal optimal control of the Cartesian 3D-crane that involves from an initial position $(0, 0, -10)$ lift the payload, track the trolley and move the bridge simultaneously to a final state at position $(10, 15, -20)$ in 20 s. In order to obtain the goal we apply iteratively the saddle point method presented in Eqs. (16)–(25), fixing $\alpha = 1 \times 10^{-11}$, and after 1000000 of iteration we have:

$$\mathbf{x}_0 = \left[0.00\ 0.02\ 0.00\ 0.01\ 1.58\ 0.00\right.$$
$$\left.-0.02\ -0.01\ 9.99\ 0.01\right]^\intercal$$
$$\mathbf{x}_1 = \left[10.00\ 0.01\ 14.99\ -0.01\ 1.57\ 0.00\right.$$
$$\left.0.00\ 0.00\ 20.00\ -0.01\right]^\intercal$$

In Figs. 2 and 3 are presented the convergence of the states and the signal control applied to the crane.

Based on the initial and final conditions of the dynamical system, we consider an open-loop control such that the state of the system can be moved to a neighborhood of the equilibrium state corresponding to the given final condition which is sensible to imprecision and uncertainty consequence of moving the trolley and the bridge. To solve this problem we will introduce an ISMC to suppress the model imprecision and uncertainty consequence of moving the trolley and the bridge, as well as lifting the cargo.

5 ISMC for the 3D-crane

5.1 Design of the ISMC

The dynamical system is affected by uncertainties. We propose to employ an integral sliding mode control to compensate the uncertainties [11]. To add initial perturbations to the dynamical system, let us split the function $f\left(\mathbf{x}(t), \mathbf{u}(t)\right)$ as follows:

$$f\left(\mathbf{x}(t), \mathbf{u}(t)\right) = g\left(\mathbf{x}(t)\right) + B\left(\mathbf{x}(t)\right)\mathbf{u}(t)$$

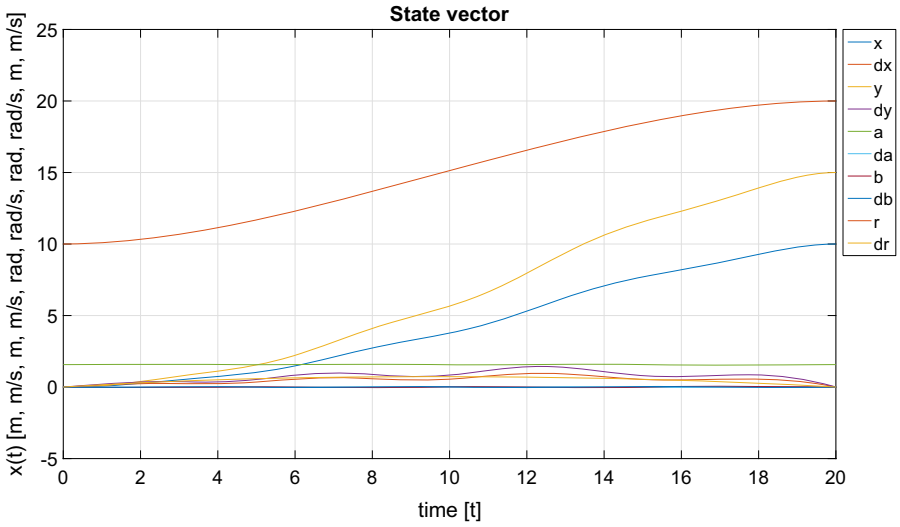

Fig. 2 Trajectory of the state vector

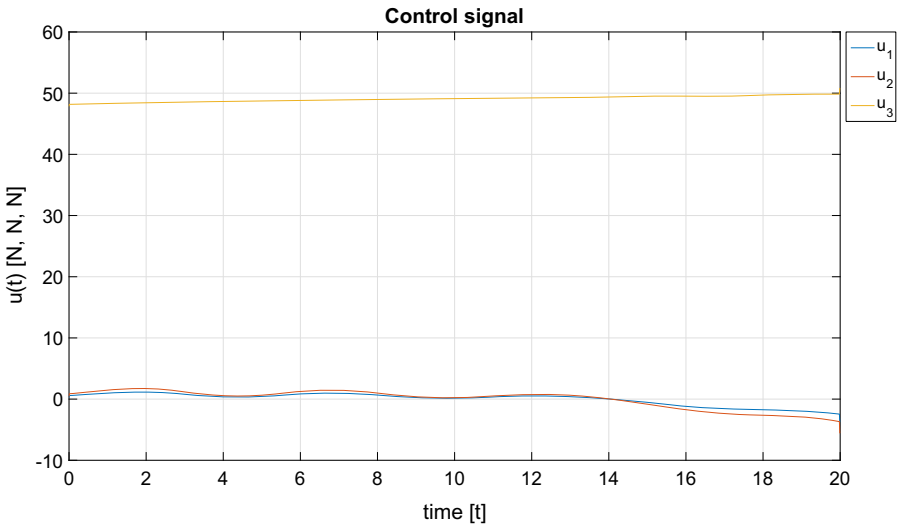

Fig. 3 Control signal obtained via saddle point method

where

$$B(\mathbf{x}(t)) = \begin{bmatrix} 0 & 0 & 0 \\ \frac{1}{m_w} & 0 & \frac{\cos\alpha}{m_w} \\ 0 & 0 & 0 \\ 0 & \frac{1}{m_w} & \frac{\sin\alpha\sin\beta}{m_w} \\ 0 & 0 & 0 \\ \frac{\sin\alpha}{rm_w} & -\frac{\cos\alpha\sin\beta}{rm_w} & \frac{\cos\alpha\cos^2\beta\sin\alpha}{rm_w} \\ 0 & 0 & 0 \\ 0 & -\frac{\cos\beta}{rm'_w\sin\alpha} & -\frac{\cos\beta\sin\alpha\sin\beta}{rm_w\sin\alpha} \\ 0 & 0 & 0 \\ -\frac{\cos\alpha}{m_w} & -\frac{\sin\alpha\sin\beta}{m_w} & -\frac{m_c+m_w-m_c\cos^2\beta+m_c\cos^2\alpha\cos^2\beta}{m_c m_w} \end{bmatrix}$$

and $g(\mathbf{x}(t)) : \mathbb{R}^n \to \mathbb{R}^n$.

Then, let us consider the following controlled uncertain system represented by the state space equation given by

$$\dot{\mathbf{x}}(t) = g(\mathbf{x}(t)) + B(\mathbf{x}(t))\,\mathbf{u}(t) + \phi(\mathbf{x}(t), t) \tag{35}$$

where the function $\phi(\mathbf{x}(t), t)$ represents the uncertainties affecting the system due to parameter variations, unmodeled dynamics, and/or exogenous disturbances. For the control design given in Eq. (35) we assume that the uncertainty satisfies the so called match condition, namely

$$\phi(\mathbf{x}(t), t) := B(\mathbf{x}(t))\,\gamma(\mathbf{x}(t), t)$$
$$\|\gamma(\mathbf{x}(t), t)\| \leq \gamma^{+}(\mathbf{x}(t), t) \tag{36}$$

Now, the control design problem is to design a control law that provided that $\mathbf{x}(0) = \mathbf{x}_0$ guarantees the

identity $x(t) = x_t$ for all $t \geq 0$

$$\mathbf{u}(t) = \mathbf{u}_0(t) + \mathbf{u}_1(t) \tag{37}$$

where $\mathbf{u}_0(t)$ is the optimal control computed using the saddle point method and $\mathbf{u}_1(t)$ is the new integral sliding mode control for guarantying the compensation of the unmeasured matched uncertainty $\phi(\mathbf{x}(t), t)$, starting from the beginning ($t = 0$).

Since $\phi(\mathbf{x}(t), t) := B(\mathbf{x}(t))\gamma(\mathbf{x}(t), t)$ substitution of Eq. (37) into Eq. (35) yields

$$\dot{\mathbf{x}}(t) = g(\mathbf{x}(t)) + B(\mathbf{x}(t))(\mathbf{u}_0(t) + \mathbf{u}_1(t) + \gamma(\mathbf{x}(t), t))$$

The sliding manifold is given by means of the equation $s(\mathbf{x}) = 0$ with s defined by the formula

$$s(\mathbf{x}) := s_0(\mathbf{x}) - s_0(\mathbf{x}_0) - \int_0^t G(\mathbf{x}(\tau))\left[g(\mathbf{x}(\tau)) + B(\mathbf{x}(\tau))\mathbf{u}_0(\tau)\right] d\tau \tag{38}$$

where $s_0(\mathbf{x}) \in \mathbb{R}^r$ is a vector that could be designed as a linear combination of the state and $G(\mathbf{x}) = \partial s_0/\partial \mathbf{x}$. Then, in contrast with conventional sliding modes, here an integral term is included. Furthermore, in this case we have $s(\mathbf{x}(0)) = 0$.

Thus, the time derivative of s is obtained by the formula

$$\dot{s} = G(\mathbf{x})B(\mathbf{x}(t))(\mathbf{u}_1 + \gamma) \tag{39}$$

In order to achieve the sliding mode, the term s_0 should be designed such that

$$\det\left[G(\mathbf{x})B(\mathbf{x}(t))\right] \neq 0, \ \forall \mathbf{x} \in \mathbb{R}^n$$

The ISMC may be designed as

$$\begin{aligned} \mathbf{u}_1 &= -M(\mathbf{x}, t)\frac{D^{\mathsf{T}}(\mathbf{x})s}{\|D^{\mathsf{T}}(\mathbf{x})s\|} \\ &\quad M(\mathbf{x}, t) > \gamma^+(\mathbf{x}(t), t), \ D(\mathbf{x}) \\ &= G(\mathbf{x})B(\mathbf{x}(t)) \end{aligned} \tag{40}$$

For proving that the sliding mode is achieved from the beginning let us introduce the following Lemma.

Lemma 1 *Let the ISMC should be designed as in Eq.* (40). Then, the sliding mode for the dynamical system

$$f(\mathbf{x}(t), \mathbf{u}(t)) = g(\mathbf{x}(t)) + B(\mathbf{x}(t))\mathbf{u}(t)$$

is achieved from the beginning.

Proof Taking the quadratic Lyapunov-like function $V = \frac{1}{2}s^{\mathsf{T}}s$, and the restriction given in Eq. (36), the time derivative of V is $\dot{V} = \langle s, \dot{s}\rangle = \langle s, D(\mathbf{u}_1 + \gamma)\rangle = \langle D^{\mathsf{T}}s, \mathbf{u}_1 + \gamma\rangle \leq -\|D^{\mathsf{T}}s\|\left(M - \gamma^+\right) < 0$. Hence V decreases, which implies

$$V(t) \leq V(0) = \frac{1}{2}\|s(\mathbf{x}_0)\|^2 = 0$$

Now, the equivalent control $u_{1\text{eq}}$ is taken from $\dot{s} = 0$:

$$\dot{s} = \mathbf{u}_1 + \gamma = 0$$

Thus, in this case,

$$\mathbf{u}_{1_{\text{eq}}} = -\gamma \tag{41}$$

□

Equation (41) represents the dynamical equivalence of the ISMC, i.e., this control achieves the sliding manifold at the first time and holds vanished the perturbations during all time. When the sliding manifold is achieved the chattering effect presents: A high- frequency on–off control signal (non smooth) is active in the actuators of the crane.

5.2 Numerical example: ISMC

Considering the controlled uncertain system represented by Eq. (35) and a perturbation, it is applied an ISMC with the form

$$\begin{aligned} s_0(\mathbf{x}(t)) &:= B(\mathbf{x}(t))^{\mathsf{T}}\mathbf{x}(t) \\ G(\mathbf{x}(t)) &:= B(\mathbf{x}(t))^{\mathsf{T}} \\ M &:= 4 \end{aligned}$$

then, control law is given by

$$\mathbf{u}(t) = \mathbf{u}_0(t) + \mathbf{u}_1(t)$$

where

$$\mathbf{u}_1(t) := -M\frac{B^{\mathsf{T}}G^{\mathsf{T}}s(t)}{\|B^{\mathsf{T}}G^{\mathsf{T}}s(t)\|}$$

where $s(t)$ is given by Eq. (39). We choose the following perturbation at the beginning

$$\gamma(\mathbf{x}(t), t) := \begin{bmatrix} \sin(t\sin(t)) \\ \sin(2t)\sin(4t) \\ \sin(3t) \end{bmatrix}$$

which satisfy the restrictions required by the system. We assume that our actuators can respond to the high frequency of the ISMC quick enough (the frequency

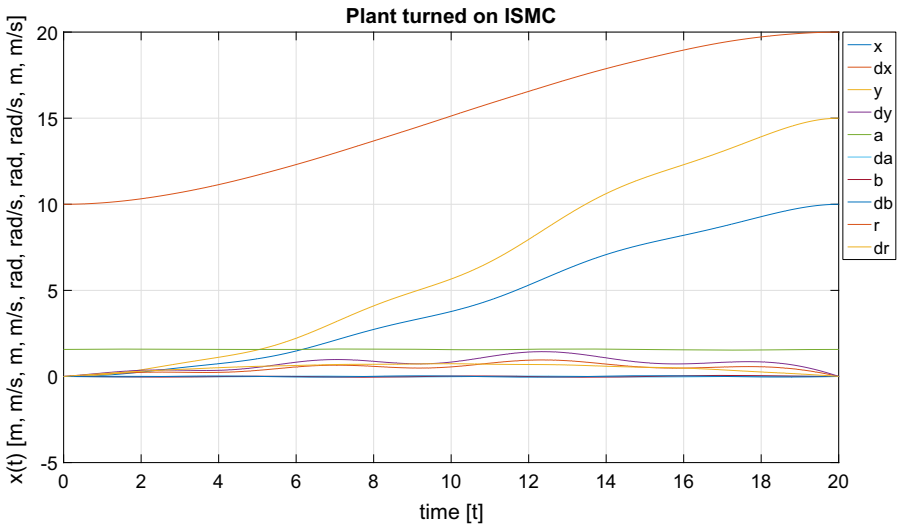

Fig. 4 State vector of the crane with turned on ISMC rejection

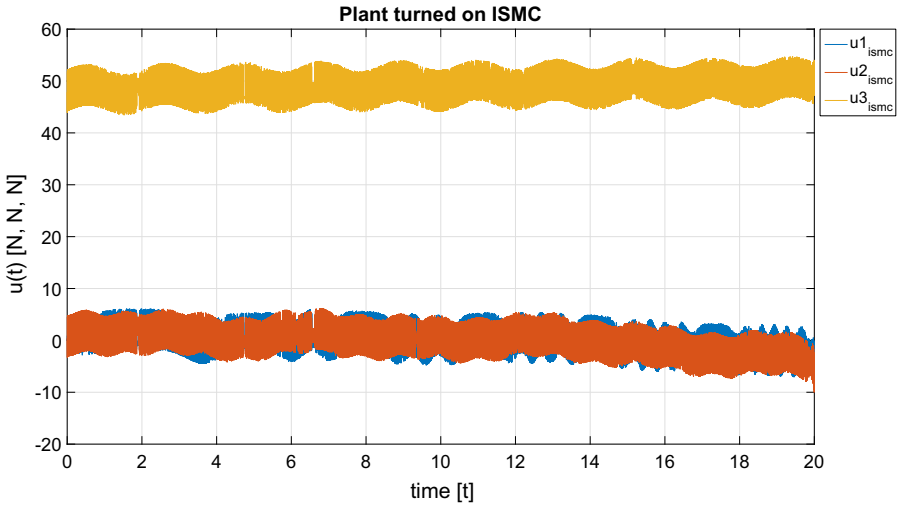

Fig. 5 Control signal with ISMC

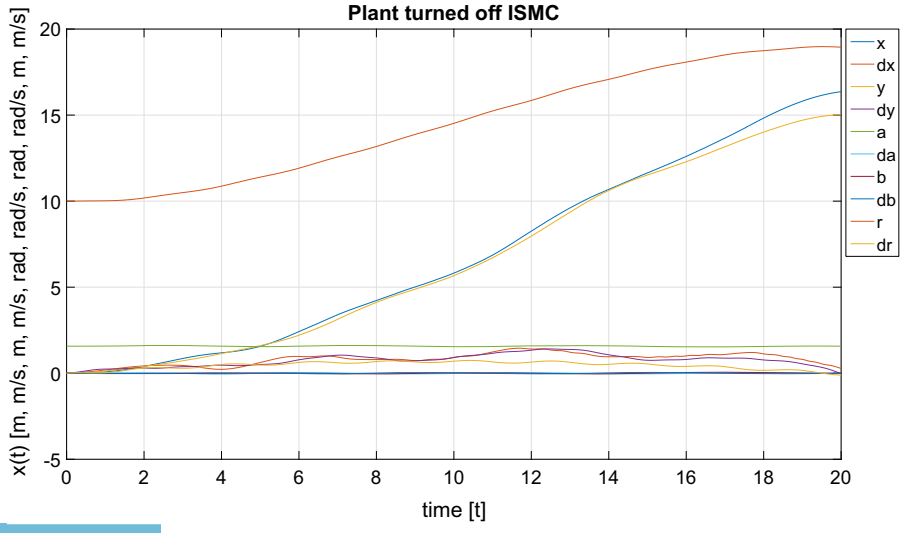

Fig. 6 State vector of the crane with turned off ISMC rejection

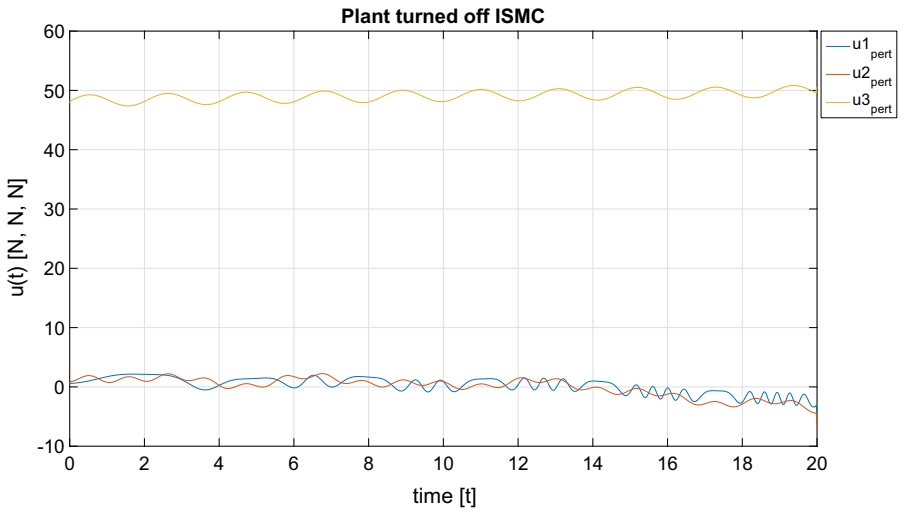

Fig. 7 Control signal without ISMC and with input perturbations

depends of the integration step, and theoretically this frequency is infinite). In the example, we employ 1×10^{-4}[s] for the integration step (a frequency of 10[kHz]).

Figures 4 and 5 show how the ISMC rejects the perturbations and the state vector holds bounded along the fixed time, and it is possible to observe that the final states do not correspond with the final states computed via the saddle point method. This is normal, because the theory assumes not discretization of the problem, but to develop a simulation of the system is necessary do it. When the manifold is achieved by the ISMC, the chattering effect is presented to very high frequencies and does not exist any computational method that can simulate this effect correctly.

Figures 6 and 7 show the effect of turned off the ISMC in the 3D-crane, and we can see the states of the system are not in the neighborhood of the fixed convex set.

6 Conclusions and future work

This paper presented a general method for controlling 3D-cranes. We developed a complete dynamical model for a Cartesian 3D-crane using the Euler–Lagrange equations, taking into account that the friction forces were not considered in the model. A controller was designed using a terminal optimal control and an ISMC technique for tracking control. For designing the optimal control for a fixed time we extended the saddle point method for controllable nonlinear dynamical systems. We implemented an ISMC for rejecting input-bounded matched disturbances. Movement of the trolley and its stoppage were controlled precisely at its destination. The control worked well and stabilized the overall crane system. Using a quadratic Lyapunov-like function we proved that the sliding mode for the 3D-crane is achieved from the beginning.

In terms of future work, there exist a number of challenges left to address. One interesting technical challenge is that of addressing an optimal feedback control via extending the saddle point method. In the short time, we are planning to apply the method for designing a sophisticated control for different and more complicated pendulum problems. It also would be interesting in the long time to extend the method in the context of game theory for modeling a dynamical game approach.

Appendix: Proof of Theorem 1

Proof The main effort in the theorem is placed on the proof of the fact that the function $\left\|\mathbf{u}^k(\cdot) - \mathbf{u}^*(\cdot)\right\|^2 + \left|p_0^k - p_0^*\right|^2 + \left|p_1^k - p_1^*\right|^2 + \left|\mathbf{x}_0^k - \mathbf{x}_0^*\right|^2$ decreases monotonically. For this, we use the variational inequalities. From Eqs. (23) and (8) written in variational inequalities, summing and using the integrations by parts formula, and using the monotonicity formula (2) for the operator $\nabla\varphi_1(\mathbf{x}_1)$ and combining like terms, we obtain the inequality:

$$\epsilon\left\langle A_1^{\mathsf{T}}\left(\bar{p}_1 - p_1^*\right), \mathbf{x}_1^* - \bar{\mathbf{x}}_1^k\right\rangle - \left\langle \bar{\Psi}_0^k - \Psi_0^*, \mathbf{x}_0^* - \bar{\mathbf{x}}_0^k\right\rangle$$

$$+\epsilon\int_{t_0}^{t_f}\left\langle\bar{\Psi}^k(t)-\Psi^*(t),\frac{\partial f}{\partial\mathbf{x}}\left(\mathbf{x}^*(t)-\bar{\mathbf{x}}^k(t)\right)\right.$$
$$\left.-\frac{\mathrm{d}}{\mathrm{d}t}\left(\mathbf{x}^*(t)-\bar{\mathbf{x}}^k(t)\right)\right\rangle\mathrm{d}t\geq 0 \tag{42}$$

Similar estimates are derived with respect to p_0 and p_1. To this end, we set:

$$\left\langle\bar{p}_0^k-p_0^k-\epsilon\left(A_0\mathbf{x}_0^k-a_0\right),p_0^{k+1}-\bar{p}_0^k\right\rangle\geq 0$$

and developing, we get:

$$\left\langle\bar{p}_0^k-p_0^k,p_0^{k+1}-\bar{p}_0^k\right\rangle+\left\langle p_0^{k+1}-p_0^k,p_0^*-p_0^{k+1}\right\rangle$$
$$+\left\langle\bar{p}_1^k-p_1^k,p_1^{k+1}-\bar{p}_1^k\right\rangle+\left\langle p_1^{k+1}-p_1^k,p_1^*-p_1^{k+1}\right\rangle$$
$$+\epsilon^2\|A_0\|^2|\bar{\mathbf{x}}_0^k-\mathbf{x}_0^k|^2-\epsilon\left\langle A_0\left(\bar{\mathbf{x}}_0^k-\mathbf{x}_0^*\right),p_0^*-\bar{p}_0^k\right\rangle$$
$$-\left\langle\bar{\Psi}_0^k-\Psi_0^*,\mathbf{x}_0^*-\bar{\mathbf{x}}_0^k\right\rangle$$
$$+\epsilon\int_{t_0}^{t_f}\left\langle\bar{\Psi}^k(t),\frac{\partial f}{\partial\mathbf{x}}\left(\mathbf{x}^*(t)-\bar{\mathbf{x}}^k(t)\right)\right.$$
$$\left.-\frac{\mathrm{d}}{\mathrm{d}t}\left(\mathbf{x}^*(t)-\bar{\mathbf{x}}^k(t)\right)\right\rangle\mathrm{d}t\geq 0 \tag{43}$$

Let us derive similar estimates with respect to controls:

$$\int_{t_0}^{t_f}\left\langle\bar{\mathbf{u}}^k(t)-\mathbf{u}^k(t)+\epsilon\frac{\partial f}{\partial\mathbf{u}}^{\mathsf{T}}(t)\Psi^k(t),\right.$$
$$\left.\mathbf{u}^{k+1}(t)-\bar{\mathbf{u}}^k(t)\right\rangle\mathrm{d}t\geq 0$$

and developing, we have:

$$\int_{t_0}^{t_f}\langle\bar{\mathbf{u}}^k(t)-\mathbf{u}^k(t),\mathbf{u}^{k+1}(t)-\bar{\mathbf{u}}^k(t)\rangle\mathrm{d}t$$
$$+\int_{t_0}^{t_f}\langle\mathbf{u}^{k+1}(t)-\mathbf{u}^k(t),\mathbf{u}^*(t)-\mathbf{u}^{k+1}(t)\rangle\mathrm{d}t$$
$$-\epsilon\int_{t_0}^{t_f}\langle\frac{\partial f}{\partial\mathbf{u}}^{\mathsf{T}}\left(\bar{\Psi}^k(t)-\Psi^k(t)\right),\mathbf{u}^{k+1}(t)-\bar{\mathbf{u}}^k(t)\rangle\mathrm{d}t$$
$$+\epsilon\int_{t_0}^{t_f}\langle\bar{\Psi}^k(t)-\Psi^*(t),\frac{\partial f}{\partial\mathbf{u}}\left(\mathbf{u}^*(t)-\bar{\mathbf{u}}^k(t)\right)\rangle$$
$$\mathrm{d}t\geq 0 \tag{44}$$

Summing up (43) and (44) and considering:

$$\frac{\partial f}{\partial\mathbf{x}}\left(\mathbf{x}^*(t)-\bar{\mathbf{x}}^k(t)\right)+\frac{\partial f}{\partial\mathbf{u}}\left(\mathbf{u}^*(t)-\bar{\mathbf{u}}^k(t)\right)$$
$$-\frac{\mathrm{d}}{\mathrm{d}t}\left(\mathbf{x}^*(t)-\bar{\mathbf{x}}^k(t)\right)=0 \tag{45}$$

we obtain:

$$\langle\bar{p}_0^k-p_0^k,p_0^{k+1}-\bar{p}_0^k\rangle+\langle p_0^{k+1}-p_0^k,p_0^*-p_0^{k+1}\rangle$$
$$+\langle\bar{p}_1^k-p_1^k,p_1^{k+1}-\bar{p}_1^k\rangle+\langle p_1^{k+1}-p_1^k,p_1^*-p_1^{k+1}\rangle$$
$$+\epsilon^2\|A_0\|^2|\bar{\mathbf{x}}_0^k-\mathbf{x}_0^k|^2-\epsilon\langle A_0\left(\bar{\mathbf{x}}_0^k-\mathbf{x}_0^*\right),p_0^*-\bar{p}_0^k\rangle$$
$$-\epsilon\langle\bar{\Psi}_0^k-\Psi_0^*,\mathbf{x}_0^*-\bar{\mathbf{x}}_0^k\rangle$$
$$+\int_{t_0}^{t_f}\langle\bar{\mathbf{u}}^k(t)-\mathbf{u}^k(t),\mathbf{u}^{k+1}(t)-\bar{\mathbf{u}}^k(t)\rangle\mathrm{d}t$$
$$+\int_{t_0}^{t_f}\langle\mathbf{u}^{k+1}(t)-\mathbf{u}^k(t),\mathbf{u}^*(t)-\mathbf{u}^{k+1}(t)\rangle\mathrm{d}t$$
$$-\epsilon\int_{t_0}^{t_f}\langle\frac{\partial f}{\partial\mathbf{u}}^{\mathsf{T}}\left(\bar{\Psi}^k(t)-\Psi^k(t)\right),$$
$$\mathbf{u}^{k+1}(t)-\bar{\mathbf{u}}^k(t)\rangle\mathrm{d}t\geq 0$$

Similarly, we can develop analogous estimates with respect to $\mathbf{x}_0$, obtaining the equation:

$$\langle\bar{p}_0^k-p_0^k,p_0^{k+1}-\bar{p}_0^k\rangle+\langle p_0^{k+1}-p_0^k,p_0^*-p_0^{k+1}\rangle$$
$$+\langle\bar{p}_1^k-p_1^k,p_1^{k+1}-\bar{p}_1^k\rangle+\langle p_1^{k+1}-p_1^k,p_1^*-p_1^{k+1}\rangle$$
$$+\epsilon^2\|A_0\|^2|\bar{\mathbf{x}}_0^k-\mathbf{x}_0^k|^2+\epsilon^2\|A_1\|^2|\bar{\mathbf{x}}_1^k-\mathbf{x}_1^k|^2$$
$$+\langle\bar{\mathbf{x}}_0^k-\mathbf{x}_0^k,\mathbf{x}_0^{k+1}-\bar{\mathbf{x}}_0^k\rangle+\langle\mathbf{x}_0^{k+1}-\mathbf{x}_0^k,\mathbf{x}_0^*-\mathbf{x}_0^{k+1}\rangle$$
$$+\int_{t_0}^{t_f}\langle\bar{\mathbf{u}}^k(t)-\mathbf{u}^k(t),\mathbf{u}^{k+1}(t)-\bar{\mathbf{u}}^k(t)\rangle\mathrm{d}t$$
$$+\int_{t_0}^{t_f}\langle\mathbf{u}^{k+1}(t)-\mathbf{u}^k(t),\mathbf{u}^*(t)-\mathbf{u}^{k+1}(t)\rangle\mathrm{d}t$$
$$-\epsilon\int_{t_0}^{t_f}\langle\frac{\partial f}{\partial\mathbf{u}}^{\mathsf{T}}\left(\bar{\Psi}^k(t)-\Psi^k(t)\right),\mathbf{u}^{k+1}(t)-\bar{\mathbf{u}}^k(t)\rangle\mathrm{d}t$$
$$+\epsilon\langle\nabla\varphi_0\left(\mathbf{x}_0^k\right)-\nabla\varphi_0\left(\bar{\mathbf{x}}_0^k\right),\mathbf{x}_0^{k+1}-\bar{\mathbf{x}}_0^k\rangle$$
$$+\epsilon\langle A_0^{\mathsf{T}}\left(p_0^k-\bar{p}_0^k\right),\mathbf{x}_0^{k+1}-\bar{\mathbf{x}}_0^k\rangle$$
$$+\epsilon\langle\Psi_0^k-\bar{\Psi}_0^k,\mathbf{x}_0^{k+1}-\bar{\mathbf{x}}_0^k\rangle\geq 0 \tag{46}$$

By using the identity $|y_1-y_2|^2=|y_1-y_3|^2+2\langle y_1-y_3,y_3-y_2\rangle+|y_3-y_2|^2$, the scalar products in (46) are decomposed into the sum (difference) of squares:

$$|p_0^{k+1}-p_0^*|^2+|p_0^{k+1}-\bar{p}_0^k|^2+|\bar{p}_0^k-p_0^k|^2$$
$$+|p_1^{k+1}-p_1^*|^2+|p_1^{k+1}-\bar{p}_1^k|^2+|\bar{p}_1^k-p_1^k|^2$$
$$-2\epsilon^2\|A_0\|^2|\bar{\mathbf{x}}_0^k-\mathbf{x}_0^k|^2-2\epsilon^2\|A_1\|^2|\bar{\mathbf{x}}_1^k-\mathbf{x}_1^k|^2$$
$$+\|\mathbf{u}^{k+1}(\cdot)-\mathbf{u}^*(\cdot)\|^2+\|\mathbf{u}^{k+1}(\cdot)-\bar{\mathbf{u}}^k(\cdot)\|^2 \tag{47}$$

$$
\begin{aligned}
&+\|\bar{\mathbf{u}}^k(\cdot)-\mathbf{u}^k(\cdot)\|^2\\
&+2\epsilon\int_{t_0}^{t_f}\langle\frac{\partial f}{\partial \mathbf{u}}^{\mathsf{T}}\left(\bar{\Psi}^k(t)-\Psi^k(t)\right),\mathbf{u}^{k+1}(t)-\bar{\mathbf{u}}^k(t)\rangle \mathrm{d}t\\
&+|\mathbf{x}_0^{k+1}-\mathbf{x}_0^*|^2+|\mathbf{x}_0^{k+1}-\bar{\mathbf{x}}_0^k|^2+|\bar{\mathbf{x}}_0^k-\mathbf{x}_0^k|^2\\
&+2\epsilon\langle\nabla\varphi_0\left(\mathbf{x}_0^k\right)-\nabla\varphi_0\left(\bar{\mathbf{x}}_0^k\right),\mathbf{x}_0^{k+1}-\bar{\mathbf{x}}_0^k\rangle\\
&+2\epsilon\langle A_0^{\mathsf{T}}\left(p_0^k-\bar{p}_0^k\right),\mathbf{x}_0^{k+1}-\bar{\mathbf{x}}_0^k\rangle\\
&+2\epsilon\langle\Psi_0^k-\bar{\Psi}_0^k,\mathbf{x}_0^{k+1}-\bar{\mathbf{x}}_0^k\rangle\leq|p_0^k-p_0^*|^2\\
&+|p_1^k-p_1^*|^2+\|\mathbf{u}^k(\cdot)-\mathbf{u}^*(\cdot)\|^2+|\mathbf{x}_0^k-\mathbf{x}_0^*|^2
\end{aligned}
$$

The scalar products on the left-hand side of (47) are estimated separately. From the equations of the algorithm, it is possible to obtain obvious inequalities and:

$$
\begin{aligned}
&\int_{t_0}^{t_f}\left\langle\frac{\partial f}{\partial \mathbf{u}}^{\mathsf{T}}\left(\bar{\Psi}^k(t)-\Psi^k(t)\right),\mathbf{u}^{k+1}(t)-\bar{\mathbf{u}}^k(t)\right\rangle \mathrm{d}t\\
&\leq B_{\max}\|\bar{\Psi}^k(\cdot)-\Psi^k(\cdot)\|\|\mathbf{u}^{k+1}(\cdot)-\bar{\mathbf{u}}^k(\cdot)\|\\
&\leq B_{\max}^2\|\bar{\Psi}^k(\cdot)-\Psi^k(\cdot)\|^2\\
&\leq\frac{\epsilon^2B_{\max}^2\left(\exp\left(2D_{\max}t_f-t_0\right)-1\right)}{D_{\max}\left(L_1|\mathbf{x}_1^k-\bar{\mathbf{x}}_1^k|+\|A_1^{\mathsf{T}}\||p_1^k-\bar{p}_1^k|\right)^2}\\
&\leq\frac{2\epsilon^2B_{\max}^2\left(\exp\left(2D_{\max}t_f-t_0\right)-1\right)}{D_{\max}\left(L_1^2|\mathbf{x}_1^k-\bar{\mathbf{x}}_1^k|^2+\|A_1^{\mathsf{T}}\|^2|p_1^k-\bar{p}_1^k|^2\right)}\\
&=\epsilon^2d_1|\mathbf{x}_1^k-\bar{\mathbf{x}}_1^k|^2+\epsilon^2|p_1^k-\bar{p}_1^k|^2
\end{aligned}
$$

where

$$
\begin{aligned}
&B_{\max}=\max\|\frac{\partial f}{\partial \mathbf{u}}\|,\ D_{\max}=\max\|\frac{\partial f}{\partial \mathbf{x}}\|\\
&d_1=\frac{2L_1^2B_{\max}^2\left(\exp\left(2D_{\max}t_f-t_0\right)-1\right)}{D_{\max}}\\
&d_2=\frac{2\|A_1^{\mathsf{T}}\|B_{\max}^2\left(\exp\left(2D_{\max}t_f-t_0\right)-1\right)}{D_{\max}}
\end{aligned}
$$

By Lipschitz condition and the inequality $2|a||b|\leq a^2+b^2$, we obtain:

$$
\begin{aligned}
&|\Psi_0^k-\bar{\Psi}_0^k|^2\\
&\leq 2\exp\left(2D_{\max}\left(t_f-t_0\right)\right)\\
&\quad\left(L_1^2|\mathbf{x}_1^k-\bar{\mathbf{x}}_0^k|^2+\|A_1^{\mathsf{T}}\|^2|p_1^2-\bar{p}_1^k|^2\right)\\
&=d_3|\mathbf{x}_1^k-\bar{\mathbf{x}}_0^k|^2+d_4|p_1^2-\bar{p}_1^k|^2
\end{aligned}
$$

where

$$
\begin{aligned}
&d_3=2L_1^2\exp\left(2D_{\max}\left(t_f-t_0\right)\right)\\
&d_4=2\|A_1^{\mathsf{T}}\|^2\exp\left(2D_{\max}\left(t_f-t_0\right)\right)
\end{aligned}
$$

Then, the inequality (47), after combining terms, becomes:

$$
\begin{aligned}
&|p_1^{k+1}-p_1^*|^2+|p_0^{k+1}-p_0^*|^2+\|\mathbf{u}^{k+1}(\cdot)-\mathbf{u}^*(\cdot)\|^2\\
&\quad+|\mathbf{x}_0^{k+1}-\mathbf{x}_0^*|^2+|p_1^{k+1}-\bar{p}_1^k|^2+|p_0^{k+1}-\bar{p}_0^k|^2\\
&\quad+\|\bar{\mathbf{u}}^k(\cdot)-\mathbf{u}^{k+1}(\cdot)\|^2+(1-\epsilon\gamma_3)|\bar{p}_1^k-p_1^k|^2\\
&\quad+(1-\epsilon\gamma_5)|\bar{p}_0^k-p_0^k|^2+(1-\epsilon\gamma_2)|\mathbf{x}_0^{k+1}-\bar{\mathbf{x}}_0^k|^2\\
&\quad+(1-\epsilon\gamma_4)\|\mathbf{u}^k(\cdot)-\bar{\mathbf{u}}^k(\cdot)\|^2\leq\\
&|p_1^k-p_1^*|^2+\|\mathbf{u}^k(\cdot)-\mathbf{u}^*(\cdot)\|^2+|\mathbf{x}_0^k-\mathbf{x}_0^*|^2
\end{aligned}
\tag{48}
$$

where

$$
\begin{aligned}
&\gamma_1=d_4+\epsilon d_2\\
&\gamma_2=1+L_0+\|A_0^{\mathsf{T}}\|\\
&\gamma_3=2\epsilon\|A_0\|^2+L_0+\left(\epsilon d_1+d_3+2\epsilon\|A_1\|^2\right)d_6\\
&\gamma_4=\left(\epsilon d_1+d_3+2\epsilon\|A_1\|^2\right)d_5\\
&\gamma_5=\|A_0^{\mathsf{T}}\|
\end{aligned}
$$

By choosing ϵ so that:

$$
0<\epsilon<\min\left\{\frac{1}{\gamma_1},\frac{1}{\gamma_2},\frac{1}{\gamma_3},\frac{1}{\gamma_4},\frac{1}{\gamma_5}\right\}
\tag{49}
$$

all terms in (48) can be made strictly positive. Omitting all lines on the left-hand side of the inequality, except for the first and last, we obtain:

$$
\begin{aligned}
&|p_1^{k+1}-p_1^*|^2+|p_0^{k+1}-p_0^*|^2+\|\mathbf{u}^{k+1}(\cdot)-\mathbf{u}^*(\cdot)\|^2\\
&\quad+|\mathbf{x}_0^{k+1}-\mathbf{x}_0^*|^2\\
&\leq|p_1^k-p_1^*|^2+\|\mathbf{u}^k(\cdot)-\mathbf{u}^*(\cdot)\|^2+|\mathbf{x}_0^k-\mathbf{x}_0^*|^2
\end{aligned}
\tag{50}
$$

which means that the sequence:

$$
\begin{aligned}
&\Big\{|p_1^{k+1}-p_1^*|^2+|p_0^{k+1}-p_0^*|^2+\|\mathbf{u}^{k+1}(\cdot)-\mathbf{u}^*(\cdot)\|^2\\
&\quad+|\mathbf{x}_0^{k+1}-\mathbf{x}_0^*|^2\Big\}
\end{aligned}
$$

decreases monotonically on the Cartesian product $\mathbb{R}_+^m\times\mathbb{R}_+^m\times L_2^r[t_0,t_f]\times\mathbb{R}^n$.

Summing (48) from $k=0$ to $k=N$ and using the condition (49) implies the boundedness of the sequence for any N,

$$
\begin{aligned}
&|p_1^{N+1}-p_1^*|^2+|p_0^{N+1}-p_0^*|^2+\|\mathbf{u}^{N+1}(\cdot)-\mathbf{u}^*(\cdot)\|^2\\
&\quad+|\mathbf{x}_0^{N+1}-\mathbf{x}_0^*|^2\\
&\leq|p_1^0-p_1^*|^2+\|\mathbf{u}^0(\cdot)-\mathbf{u}^*(\cdot)\|^2+|\mathbf{x}_0^0-\mathbf{x}_0^*|^2
\end{aligned}
$$

and the converge of the series:

$$\begin{aligned}
&\sum_{k=0}^{\infty} |p_1^{k+1} - \bar{p}_1^k|^2 < \infty, \qquad \sum_{k=0}^{\infty} |\bar{p}_1^k - p_1^k|^2 < \infty,\\
&\sum_{k=0}^{\infty} |p_0^{k+1} - \bar{p}_0^k|^2 < \infty, \qquad \sum_{k=0}^{\infty} |\bar{p}_0^k - p_0^k|^2 < \infty,\\
&\sum_{k=0}^{\infty} |\mathbf{x}_0^{k+1} - \bar{\mathbf{x}}_0^k|^2 < \infty, \qquad \sum_{k=0}^{\infty} |\bar{\mathbf{x}}_0^k - \mathbf{x}_0^k|^2 < \infty,\\
&\sum_{k=0}^{\infty} \|\bar{\mathbf{u}}^k(\cdot) - \mathbf{u}^{k+1}(\cdot)\|^2 < \infty,\\
&\sum_{k=0}^{\infty} \|\mathbf{u}^k(\cdot) - \bar{\mathbf{u}}^k(\cdot)\|^2 < \infty
\end{aligned} \tag{51}$$

Therefore:

$$\begin{aligned}
&|p_1^{k+1} - \bar{p}_1^k| \to 0 \qquad |\bar{p}_1^k - p_1^k| \to 0\\
&|p_0^{k+1} - \bar{p}_0^k| \to 0, \qquad |\bar{p}_0^k - p_0^k| \to 0,\\
&|\mathbf{x}_0^{k+1} - \bar{\mathbf{x}}_0^k| \to 0, \qquad |\bar{\mathbf{x}}_0^k - \mathbf{x}_0^k| \to 0,\\
&\|\bar{\mathbf{u}}^k(\cdot) - \mathbf{u}^{k+1}(\cdot)\| \to 0, \quad \|\mathbf{u}^k(\cdot) - \bar{\mathbf{u}}^k(\cdot)\| \to 0
\end{aligned} \tag{52}$$

Combining this with the triangle inequality, we obtain:

$$\begin{aligned}
&|p_1^{k+1} - p_1^k| \to 0 \qquad |p_0^{k+1} - p_0^k| \to 0\\
&|\mathbf{x}_0^{k+1} - \mathbf{x}_0^k| \to 0, \qquad \|\mathbf{u}^{k+1}(\cdot) - \mathbf{u}^k(\cdot)\| \to 0,\\
&|\mathbf{x}^k(\cdot) - \bar{\mathbf{x}}^k(\cdot)| \to 0, \qquad |\mathbf{x}_1^k - \bar{\mathbf{x}}_1^k| \to 0\\
&\|\Psi^k(\cdot) - \bar{\Psi}^k(\cdot)\| \to 0 \qquad k \to \infty
\end{aligned}$$

Moreover, Eq. (51) implies that the sequence is bounded, since $\left(p_0^k, p_1^k, \Psi^k(\cdot), \mathbf{x}_0^k, \mathbf{x}_1^k, \mathbf{x}^k(\cdot), \mathbf{u}^k(\cdot)\right)$ belongs to a compact set. The last means that there exists a subsequence $\left(p_0^{k_l}, p_1^{k_l}, \Psi^{k_l}(\cdot), \mathbf{x}_0^{k_l}, \mathbf{x}_1^{k_l}, \mathbf{x}^{k_l}(\cdot), \mathbf{u}^{k_l}(\cdot)\right)$ and a point defined by $\left(p_0', p_1', \Psi'(\cdot), \mathbf{x}_0', \mathbf{x}_1', \mathbf{x}'(\cdot), \mathbf{u}'(\cdot)\right)$ that is a weak limit of the subsequence. Note that, in finite-dimensional (Euclidean) spaces, the weak convergence coincides with the strong one. □

References

1. Algarni, A.Z., Moustafa, K.A.F., Nizami, J.: Optimal control of overhead cranes. Control Eng. Pract. **3**(9), 1277–1284 (1995)
2. Almutairi, N., Zribi, M.: Sliding mode control of a three dimensional overhead crane. J. Vib. Control **15**(11), 1679–1730 (2009)
3. Antipin, A.S.: Terminal control of boundary models. Comput. Math. Math. Phys. **54**(2), 275–302 (2014)
4. Bartolini, G., Pisano, A., Usai, E.: Second-order sliding mode control of container cranes. Automatica **38**(10), 1783–1790 (2002)
5. Bartolini, G., Pisano, A., Usai, E.: Output-feedback control of container cranes: a comparative analysis. Asian J. Control **5**(4), 578–593 (2003)
6. Boltyanski, V., Poznyak, A.S.: The Robust Maximum Principle: Theory and Applications. Birkhauser, Springer, New York (2011)
7. Chang, C.Y., Chiang, K.H.: Fuzzy projection control law and its application to the overhead crane. Mechatronics **18**, 607–615 (2008)
8. Chen, Y., Wang, W., Chang, C.: Guaranteed cost control for an overhead crane with practical constraints: fuzzy descriptor system approach. Eng. Appl. Artif. Intell. **22**(4–5), 639–645 (2009)
9. Cho, S.K., Lee, H.H.: A fuzzy-logic anti-swing controller for three dimensional overhead cranes. ISA Trans. **41**, 235–243 (2002)
10. Daqaq, M.F., Masoud, Z.N.: Nonlinear input-shaping controller for quay-side container cranes. Nonlinear Dyn. **45**(1), 149–170 (2006)
11. Fridman, L., Poznyak, A.S., Bejarano, F.J.: Robust Output LQ Optimal Control via Integral Sliding Modes. Birkhauser, Springer, New York (2014)
12. Giua, A., Sanna, M., Seatzu, C.: Observer-controller design for three dimensional overhead cranes using time-scaling. Math. Comput. Model. Dyn. Syst. **7**(1), 77–107 (2001)
13. Hsu, C., Lee, T., Tanaka, K.: Intelligent nonsingular terminal sliding-mode control via perturbed fuzzy neural network. Eng. Appl. Artif. Intell. **45**, 339–349 (2015)
14. Hyla, P.: The crane control systems: a survey. In: 17th IFAC International Conference on Methods and Models in Automation and Robotics, pp. 505–509. Miedzyzdroje, Poland (2012)
15. Karkoub, M., Zribi, M.: Robust control schemes for an overhead crane. J. Vib. Control **7**, 395–416 (2001)
16. Laghrouche, S., Plestan, F., Glumineau, A.: Higher order sliding mode control based on integral sliding mode. Automatica **3**(43), 531–537 (2007)
17. Lee, H.H., Liang, Y., Segura, D.: A sliding mode anti-swing trajectory control for overhead cranes with high-speed load hoisting. J. Dyn. Syst. Meas. Control **128**(4), 842–845 (2006)
18. Liu, D., Yi, J., Zhao, D., Wang, W.: Adaptive sliding mode fuzzy control for a two dimensional overhead crane. Mechatronics **15**(5), 505–522 (2004)
19. Maghsoudi, M., Mohamed, Z., Husain, A.R., Tokhi, M.O.: An optimal performance control scheme for a 3d crane. Mech. Syst. Signal Process. **66–67**, 756–768 (2016)
20. Ngo, Q., Hong, K.S.: Sliding mode anti-sway control of an offshore container crane. IEEE/ASME Trans. Mechatron. **17**(2), 201–209 (2012)
21. Park, M.S., Chwa, D.K., Hong, S.K.: Antisway tracking control of overhead cranes with system uncertainty and actuator nonlinearity using an adaptive fuzzy sliding-mode control. IEEE Trans. Ind. Electron. **55**(11), 3972–3984 (2008)
22. Poznyak, A.S.: Advance Mathematical Tools for Automatic Control Engineers. Vol 2 Deterministic Techniques, vol 1. Elsevier, Amsterdam (2008)
23. Qian, S., Zi, B., Ding, H.: Dynamics and trajectory tracking control of cooperative multiple mobile cranes. Nonlinear Dyn. **83**(1), 89–108 (2016)

24. Sakawa, Y., Sano, H.: Nonlinear model and linear robust control of overhead travelling cranes. Nonlinear Anal. Theory Methods Appl. **30**(4), 2197–2207 (1997)
25. Shtessel, Y., Kaveh, P., Ashrafi, A.: Robust harmonic oscillator control via integral and high order sliding modes. In: 8th International Workshop on Variable Structure Systems, Spain, cD ROM (2004)
26. Smoczek, J., Szpytko, J.: Evolutionary algorithm-based design of a fuzzy tbf predictive model and tsk fuzzy anti-sway crane control system. Eng. Appl. Artif. Intell. **28**, 190–200 (2014)
27. Sun, N., Fang, Y., Chen, H.: Adaptive antiswing control for cranes in the presence of rail length constraints and uncertainties. Nonlinear Dyn. **81**, 41–51 (2015)
28. Utkin, V., Chang, H.: Sliding mode control on electromechanical systems. Math. Probl. Eng. **8**(4–5), 451–473 (2002)
29. Utkin, V., Shi, J.: Integral sliding mode in systems operating under uncertainty conditions. In: in Proceedings of the 35th IEEE Conference Decision Control, pp. 4591–4596. Kobe, Japan (1996)
30. Utkin, V., Guldner, J., Shi, J.: Sliding Mode Control in Electromechanical Systems. Taylor and Francis, London (1999)
31. Wu, Z., Xia, X., Zhu, B.: Model predictive control for improving operational efficiency of overhead cranes. Nonlinear Dyn. **79**, 2639–2657 (2015)
32. Xu, J.X., Abidi, K.: On the discrete-time integral sliding-mode control. IEEE Trans. Autom. Control **52**(4), 709–715 (2007)
33. Xu, J.X., Cao, W.: Nonlinear integral-type sliding surface for both matched and unmatched uncertain systems. In: In Proceedings American Control Conference, Arlington, Virginia, vol. 6, pp. 4369–4374 (2001)
34. Xu, J.X., Pan, Y., Lee, T.: Analysis and design of integral sliding mode control based on Lyapunov's direct method. In: In Proceedings American Control Conference, pp. 192–196. Denver, Colorado (2003)